

# Realizing a Compact Neutron Beam Collimator for Neutron Radiography

April 24, 2019

A Major Qualifying Project

Submitted to the Faculty of Worcester Polytechnic Institute

In partial fulfillment of the requirements for the degree of

Bachelor of Science

**Written By:**

Calvin M. Downey and Jessica M. Elder

**Advised By:**

Drs. Robert D. Sisson and David C. Medich

## **Abstract**

Neutron imaging is a radiographic testing technique used for non-destructive inspection applications across multiple scientific fields. In the current work, the main objective was to design, build, and analyze a compact neutron beam collimator, used in conjunction with an Adelphi compact D(d,n)He neutron generator. Designs were based on sourced MCNP parameter optimization [1], and were built using various machining techniques including water-jet cutting, laser cutting, and CNC machining. With the realized collimator implemented into the system, the thermal neutron flux was analyzed, and suggestions were outlined for future improvements.

## Acknowledgements

We would like to thank the following individuals for their support and expertise:

- Professor David C. Medich, for his knowledge of nuclear physics and for making our MQP an enjoyable experience.
- Professor Robert D. Sisson, for his engineering wisdom and for ensuring our project came to fruition.
- Nicholas Borges, for taking the time out of his busy schedule to teach us how to operate a neutron generator.
- Alexander Hamm, for his help and flexibility when assisting us with our activation analyses.
- Tom Gravel, HydroCutters Inc., for his water-jet cutting expertise.
- The Peer Learning Assistants of Washburn Shops, notably Marek Travníkar and Karl Ehlers, for their extensive design advice and suggestions, and for their machining assistance.

Our project would not have been completed to the best of our ability without all of your help.

# Contents

<b>Abstract</b>	<b>i</b>
<b>Acknowledgements</b>	<b>ii</b>
<b>List of Acronyms and Abbreviations</b>	<b>iv</b>
<b>1 Introduction</b>	<b>1</b>
<b>2 Literature Review</b>	<b>1</b>
2.1 Particle Physics . . . . .	1
2.2 Fusion Neutron Source . . . . .	4
2.3 Neutron Radiography Applications . . . . .	6
2.4 Neutron Beam Collimator Design . . . . .	7
<b>3 Methodology</b>	<b>9</b>
3.1 Modifications to a Simulated Design . . . . .	9
3.2 Design Creation . . . . .	10
3.3 Neutron Activation Analysis . . . . .	14
<b>4 Results and Discussion</b>	<b>15</b>
4.1 Design Realization . . . . .	15
4.2 Thermal Neutron Flux Analysis . . . . .	18
<b>5 Conclusions</b>	<b>18</b>
<b>6 References</b>	<b>20</b>
<b>Appendix A: Cone Configurations</b>	<b>21</b>
<b>Appendix B: Inner Stands to Ensure Coincetricity of Divergent Collimator</b>	<b>21</b>
<b>Appendix C: Collimator Assembly</b>	<b>22</b>

## List of Acronyms and Abbreviations

Acronym/abbreviation	Definition
Al	Aluminum
Bi	Bismuth
CAM	Computer automated machining
CCD	Charge-coupled device
CNC	Computer numerically controlled
DD	Deuterium-deuterium
DT	Deuterium-tritium
.dxf	Drawing eXchange format
eV	Electronvolt
HDPE	High density polyethylene
HPGe	High purity germanium
MCNP	Monte Carlo N- Particle
MeV	Megaelectronvolt
NAA	Neutron activation analysis
NR	Neutron radiography
NSE	Nuclear science and engineering
PE	Polyethylene
PE-B	Borated polyethylene
PPC-B	Borated polypropylene carbonate
TIG	Tungsten inert gas
TNC	Thermal neutron content
TT	Tritium-tritium

# 1 Introduction

Neutron imaging, also called NR, is a radiographic testing technique that uses neutrons as opposed to photons to produce an image; NR provides similar, yet fundamentally different images than photon-based imaging methods such as X-ray imaging, which is commonly used in medical applications [2]. Neutrons have widely varying and specific attenuation properties. This enables the use of NR as a non-destructive inspection method which can be favorably applied to research and solving practical, industrial related problems [3].

The focus of this project was to develop a collimator for a portable neutron generator. Specifically, our project is aimed at improving the resolution of NR images from an Adelphi DD neutron generator source, by creating a collimator to remove scattered neutrons, which degrade image contrast. Our design was a derivative of a theoretical design which was optimized by MCNP simulations [1], and created specifically for our neutron source type.

Our collimator design focused on four main parts: a convergent moderator, a divergent collimator, a void, and shielding. The moderator was created to slow fast neutrons into thermal speeds, therefore increasing thermal neutron flux, and is made out of HDPE.<sup>1</sup> The divergent collimator was created using PPC-B, which has the ability to absorb neutrons, and limit scattering. The void was created with a vacuum sealed Al chamber, and is used to limit scattering interactions with air particles. These three components were shielded with a lead casing, to block any potential  $\gamma$ -rays and X-rays in the surrounding area. Additionally, the vacuum chamber blocked  $\beta$ -rays and ensured structural integrity for internal forces from the void [4].

We then completed NAAs to test the effectiveness of our collimator. This was carried out twice: once without the collimator in place, and once with. The results of these tests were then compared to find the increased focus in thermal neutron flux that arose from usage of our collimator. Qualitative analyses should be completed in the future to analyze image resolution: also once without the collimator and once with. These tests will show change in image resolution and required imaging time due to the collimator.

## 2 Literature Review

### 2.1 Particle Physics

Because neutrons lack electric charge, they are not susceptible to Coulombic interactions. Therefore, neutrons will only interact with the nuclei of the surrounding material due to nuclear forces [5]. To accurately determine how a beam of neutrons will interact with different types of matter, one must first understand

---

<sup>1</sup>This convergent moderator can be filled with a sapphire, silicon, or quartz crystal to further filter fast neutrons. Our design uses a void opposed to these options due to time and cost constraints. This fact was considered as a potential area for future work and improvements.

how this beam is characterized.

Neutron energy is usually indicated by eV, and is also referred to as neutron temperature. Neutron temperatures are found by fitting neutron kinetic energies to a Maxwellian–Boltzmann distribution for motion. Neutron energy distributions range from 0-0.025 eV for cold neutrons to >20 MeV for ultrafast neutrons. Neutrons produced by nuclear reactors and neutron generators are typically fast neutrons, which are 0.1-10 MeV of energy. However, these fast neutrons are often slowed to lower energy levels when used for common nuclear applications like NR, to increase the likelihood of attenuation. The process used to slow fast neutrons is called moderation, which is accomplished as neutrons react with nuclei of similar masses. For thermal NR, fast neutrons are moderated into thermal neutrons with energies of 0.025 eV [6].

Neutrons have the ability to interact with nuclei through scattering, absorption, or energy transfer. Scattering occurs by elastic or inelastic collisions, absorption by capture or fission, and energy transfer by transfer reactions. Any reaction that occurs between a nuclei and an incident neutron is dependent on the nuclide type, reaction type, and the neutron energy. The likelihood of any of these occurrences can be determined by examining microscopic cross-sections. The size of the cross-section is directly related to the probability that a neutron-nucleus reaction will occur. Microscopic cross-section is found using the equation,

$$\sigma = \frac{\mu}{N} \quad (1)$$

where  $\mu$  is an attenuation coefficient [ $m^{-1}$ ], and  $N$  is the density of the interaction particles [ $m^{-3}$ ]. Microscopic cross-section is therefore measured in  $m^2$  or barns, where one barn =  $10^{-28}m^2$  or  $10^{-24}cm^2$ . A microscopic cross-section is essentially the effective area of a nucleus with which an incident neutron will interact. The attenuation coefficient is also referred to as the macroscopic cross-section, and is equal to the density of nuclei within the effective area of interaction.

Considering a beam of neutrons with an intensity  $I_0$  that interacts with a material with  $N \frac{nuclei}{cm^3}$ , one can use micro-and-macroscopic cross-sectional areas to determine the change in beam intensity anywhere throughout the material,

$$I(x) = I_0e^{-\mu x}. \quad (2)$$

This process is commonly used during NR, as the gradual decrease in intensity can be used to determine the internal structure of an object, as shown in Figure 1.

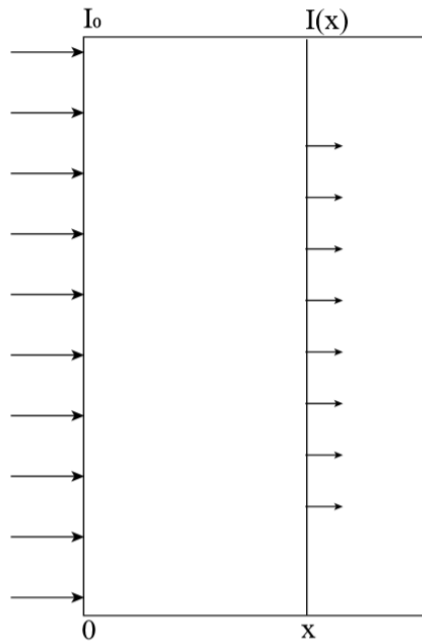


Figure 1: Beam intensity throughout a material [5]

The attenuation of a beam of radiation is dependent on the type and energy of the beam, and the type of material that it is interacting with. For example, while the radiation attenuation of X-rays and  $\gamma$ -rays increases with atomic number, attenuation of neutrons varies with each isotope, as depicted in Figure 2 .

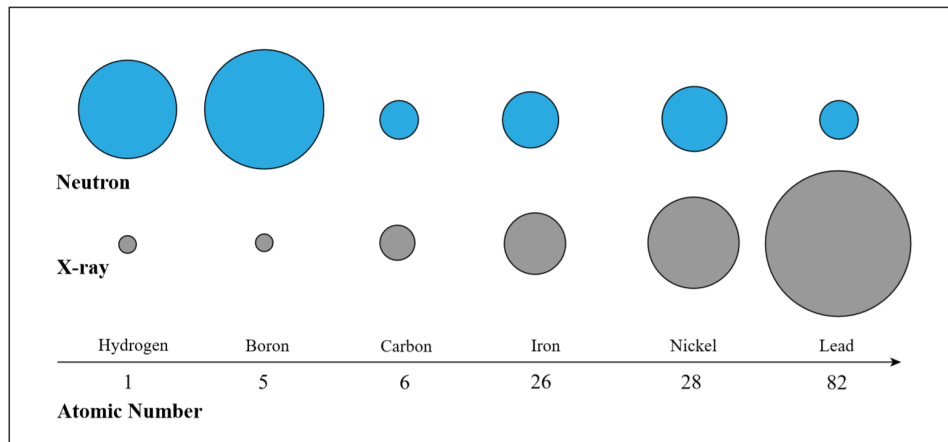


Figure 2: Relative probability of attenuation for X-rays and neutrons [2]

Unlike X-rays, neutrons interact with the nucleus opposed to orbital electrons. Therefore, the neutron's attenuation cross-sections are not related to atomic number [5].

As mentioned previously, fast neutrons are most effectively moderated using nuclei of comparable masses. This is due to elastic collisions within the material, which occur until the neutron has an energy equivalent to that of the material's. Accounting for all collisions ranging from 0 to 180°, the mean logarithmic reduction

of neutron energy per collision,  $\xi$ , can be calculated as,

$$\xi = 1 + \frac{(A - 1)^2}{2A} \ln \frac{A - 1}{A + 1} \quad (3)$$

where  $A$  is atomic mass. When graphed, this equation visually depicts the usefulness of using materials with low mass numbers as moderators (Figure 3).

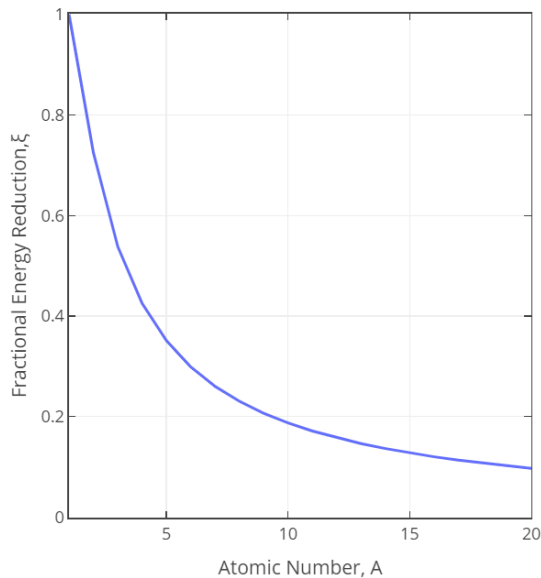


Figure 3: Logarithmic energy reduction per collision

Additionally, the number of collisions needed to slow a neutron from energy  $E_0$  to  $E_1$  can be found using the equation,

$$n = \frac{1}{\xi} (\ln E_0 - \ln E_1). \quad (4)$$

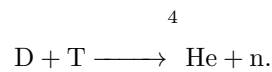
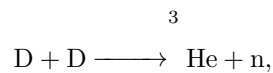
From this equation it is found that, on average, five collisions typically slow a neutron from fast to thermal energy if moderated by  $^1\text{H}$ . This number of collisions increases significantly with slight changes in mass number; for example, when  $A = 13$  (Al) over 40 collisions are needed [7].

## 2.2 Fusion Neutron Source

Neutron generation from  $\text{D}(d, n)\text{He}$  or  $\text{DD}$  fusion sources has been regularly used for the past 50 years of nuclear research and development. Most generation devices operate on relatively simplistic concepts, developed for small, modular sources, and are often used in academic settings. For this reason, neutron generator devices have become increasingly popular in NSE departments for low cost, low footprint research

and classroom demonstrations of important NSE concepts [10].

Neutron generators produce neutrons by fusing isotopes of hydrogen together to produce an isotope of helium with the release of a neutron. Deuterium gas is introduced continuously at low rates into the ion source. The desired pressure in the ion source and acceleration regions of the generator head is achieved by pumping the head with a small turbo pump. Deuterium or tritium gas is ionized by microwave radiation in Adelphi neutron generators, and held at a gas pressure of 0.1 - 0.01 mmHg. Neutrons are then produced by accelerating ionized deuterium or tritium through a high potential (125kV for DD110M) into a metal hydride, also containing deuterium or tritium [8]. The energy of the impact is enough to incite the fusion of the hydrogen isotopes, as shown by the reactions



Here, neutrons from DD fusion have 2.5 MeV of energy, and neutron from DT fusion have 14.1 MeV [9]. A magnetic field and a biased electron-shield electrode are used to prevent backscattered electrons from damaging the ion source.

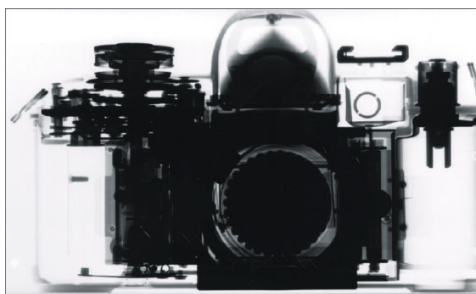
Neutron yields and fluxes of Adelphi neutron generators have been well documented and optimized with respect to varying models. Moderated generators can produce fluxes of  $10^4$  to  $10^8 \frac{\text{neutrons}}{\text{cm}^2\text{sec}}$ . Neutron yield decreases as a function of lifetime due to the depletion of deuterium or tritium atoms on the target [8]. Neutrons can be moderated, or slowed, with hydrogen bearing materials; HDPE has been shown to be an excellent and inexpensive moderator material [1]. Since the fast neutrons are emitted roughly isotropically from the deuterized titanium target, the neutrons must be slowed down in the shortest distance possible to achieve the maximum flux of thermal neutrons. MCNP simulations demonstrate that HDPE achieves a maximum thermal flux at only 5 cm from the titanium target. For this reason the outside casing of the neutron generator is lined with a 2.5 cm sheet of HDPE on the beam port end to thermalize the neutrons, and layers of borated plastic are placed on the remaining five sides of the casing to absorb neutrons.

Commercial fusion based neutron generators have a low cost and relatively short operational lifetime in comparison to conventional university research nuclear reactors [10]. Thus, it is important to effectively operate a generator during its lifetime. This is commonly done by collimating neutrons in order to focus the flux, and inherently increase the resolution of the radiographic images; collimators are therefore useful in laboratory applications where varying techniques of NR are used [1].

## 2.3 Neutron Radiography Applications

Although not as well known as X-ray radiography, NR remains an efficient non-destructive tool for many research applications. While high intensity beams of X-rays are cheaper and easier to produce than neutrons, NR remains useful for applications that cannot be imaged with X-rays or to provide complimentary information to X-rays [3]. Neutrons interact with the nuclei of the item to be imaged, rather than with the electrons, as with X-rays. Neutrons are therefore attenuated very differently than X-rays; while X-rays are stopped by heavy materials such as lead, neutrons have the ability to penetrate up to several inches of these materials [5]. NR can therefore be used to accurately image large metal objects, and can even differentiate between isotopes of an element, due to widely varying cross-sections. Neutrons also are highly attenuated by lighter materials – such as hydrogen – which makes them appealing to image smaller, more intricate biological materials containing multiple low-Z materials. Figure 4, depicts differences that can arise between X-ray imaging and NR.

a) X-ray imaging



b) Neutron imaging

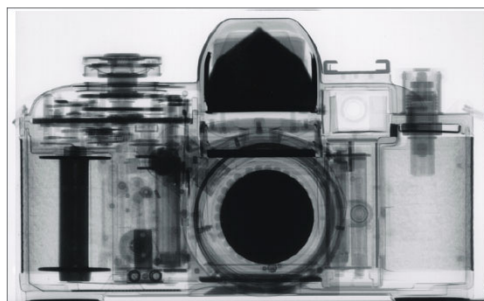


Figure 4: An example of X-ray versus neutron imaging [2]

Radiography is a two-dimensional method of imaging that entails transmitting a beam of neutrons through an object and onto a detector. This technique can then be repeated using several varying orientations of the same object to create a three-dimensional image, called tomography [11]. Uses of two-dimensional radiography and three-dimensional tomography include, but are not limited to

- imaging of biological molecules (through reconstruction of small-angle neutron scatters),
- analysis of moisture content in biological objects,
- hydrology and geology applications, through the study of rock formations,
- palaeontology applications, through fossil examination,
- examination of nuclear fuel elements, and

- materials research, through imaging alloys, welds, internal strains, etc. [3]

The setup for imaging usually includes a scintillator to detect neutrons. These scintillated light beams then hit a mirror and reflect into a CCD camera. This camera is attached to a computer, which creates the final image. The whole system is usually encased in a light-tight box to increase image resolution (Figure 5).

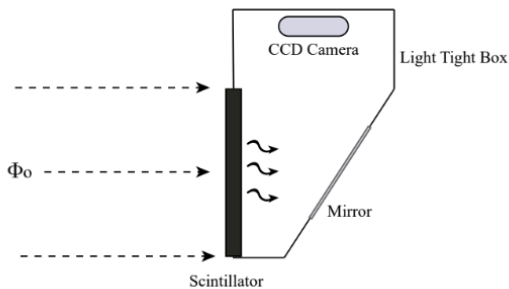


Figure 5: Neutron imaging camera setup [12]

## 2.4 Neutron Beam Collimator Design

The purpose of a neutron collimator is to slow neutrons to desired energy levels, and to minimize scattering. The basis of neutron collimator design is focused on four main components: a convergent moderator, a divergent collimator, a void, and shielding of unwanted radiation. The geometry of these components can then be modified to fit design requirements for the desired neutron beam type, which is dependent on the beam’s applications. Geometric parameters for a collimator design can then be optimized using MCNP simulations or other particle transport software. The first piece of the collimator, coincident to the neutron source is the convergent moderator. This piece usually consists of an illuminator and a fast neutron filter. The illuminator is used to obtain uniform intensity for the initial beam of neutrons, and is made of a highly neutron absorptive material, such as PE. The moderator is usually approximately 10 cm in length, and must be sized in such a way that it is long enough to slow neutrons, while not being excessively long such that the neutron flux would be reduced. The fast neutron filter is then placed inside of the convergent cone, and is typically made of a single-sapphire, silicon, or quartz crystal. Although this crystal is only used to reduce amounts of unwanted energetic neutrons, and therefore does not improve the resulting image, it can reduce the amount of fast neutron shielding that may be required for certain facilities.

Adjacent to the convergent moderator is the divergent collimator, which is the most important piece for obtaining neutron radiography properties. This part begins with an aperture, which is typically a round hole that only allows thermal neutrons to pass through its area. The aperture is therefore made of an absorptive

material and sized in accordance to a collimation ratio,  $\frac{L}{D}$ . The collimation ratio is the ratio of the divergent collimator length to the aperture diameter which gives the image resolution limit. This ratio is directly related to image resolution, and can be used to relate the neutron flux at the image plane to that at the aperture, as shown by the equations,

$$u_g = L_i \frac{D}{L_s} \quad (5)$$

$$\phi_i = \frac{\phi_\alpha}{16 \frac{L_s}{D}^2} \quad (6)$$

where  $u_g$  is geometric unsharpness (image resolution),  $L_i$  is the distance from the image surface to the imaged object,  $D$  is the aperture diameter,  $L_s$  is the distance from the particle source to the imaged object, and  $\phi_i$  and  $\phi_\alpha$  are the particle flux at the image surface and aperture, respectively. The divergent collimator must also be sized to account for beam divergence. Beam divergence is measured by its half-angle,  $\theta$ , where

$$\theta = \tan^{-1}\left(\frac{I}{2L}\right), \quad (7)$$

and where  $I$  is the maximum dimension of the imaged object and  $L$  is the length of the divergent collimator. The half-angle of beam divergence must be small enough to ensure that the outer edges of the resulting images are correctly shaped; if the neutron beam diverges too quickly then the edges of the image will be distorted. Furthermore, the walls of the collimator should be made of a borated material with high attenuation and low scattering cross-sections [1].

It is important to limit scattering within the collimator, as scattered neutrons decrease the sharpness of the image. Therefore, the collimator should be vacuum sealed as to eliminate scattering due to air particles. Scattered neutrons can also cause unwanted interactions, which require additional shielding. The most commonly used materials to block  $\gamma$ -rays are Bi and Pb, with the former having a lower and therefore more favorable neutron attenuation coefficient [14]. Additionally, the entire assembly may be cased with Al, which will block  $\beta$ -particles and will ensure structural integrity when creating a void.

## 3 Methodology

### 3.1 Modifications to a Simulated Design

The first step in this project was to identify key parameters of the neutron beam collimator. These parameters were predominantly sourced from the paper, *Fast and Thermal Neutron Radiographies Based on a Compact Neutron Generator*[1], by Fantidis, et al., published in the Journal of Theoretical and Applied Physics. In this study, MCNP4B simulations were used to quantify the flux of both thermal and fast spectrum neutrons at the image plane, with various geometric and material parameters applied to the collimator design. MCNP simulations were carried out using DD, DT, and TT neutron sources. The specific aim of this project was to design an NR system for an Adelphi DD110M neutron generator. Data used were therefore from the DD design section of the paper.

Effective neutron collimators require effective moderation, absorption, and scattering of neutrons in specific sections of the collimator. It is vital for neutrons to first be moderated before entering the collimator. In the MCNP simulations, the front of the collimator convergent moderator is covered with a 2.4 cm sheet of HDPE, to moderate the neutrons before entering the collimator. However, because the source used for this project is moderated internally, this part of the simulated collimator was omitted in project designs. For the convergent section of the collimator, the simulations completed by Fantidis et al. also identify HDPE as the material of choice for the convergent moderated section of the collimator “to provide the maximum neutron flux at the collimator inlet.” [1] The following design section – the divergent collimator – plays a large role in the neutron intensity at the exit of the collimator; it is crucial that the inner wall should be made of a material with high absorption and low scattering cross-sections. For this reason, boron was chosen as the neutron absorbing material on the lining of the collimator inner wall, with PE-B surrounding it. Due to availability and ease of manufacture, PPC-B was used as the material for the entirety of the divergent collimator section for this project, providing a similar net neutron absorption cross-section. The outside of the simulated collimator was then lined with 1 cm of Bi, to absorb  $\gamma$ -rays and scattered neutrons. Bi was used to follow health code regulations in the paper’s country of origin, so this project instead uses Pb, which is a more efficient and less expensive gamma absorber.

With the materials decided upon, it was crucial to identify the specific geometric parameters required for the specific source and application of the collimator. Primarily, for the purpose of NR, an  $\frac{L}{D}$  of 100 was set, thus requiring a total length of 1 m versus an aperture diameter of 1 cm. Fantidis et al. recommended an image plane of 16 cm in diameter, yielding a beam divergence angle of  $4.57^\circ$ . The walls of the divergent collimator were specified to be 4 cm thick. For the convergent moderator, it was recommended that the total length of the moderator be 14 cm for DD sources, rather than 15 cm as specified for DT and TT, and

that the OD of the cylinder be 13 cm. The inlet diameter of the convergent moderator began at 7 cm, and tapered to 1 cm. In the studied paper, a 1 cm Bi collimator casing was specified to absorb stray  $\gamma$ -rays which may enter the image plane externally from the system from random activations in the neutron source room. We decided to use Pb in the same capacity as Bi, due to availability and improved  $\gamma$ -ray shielding. It was imperative to be certain that these geometric parameters were followed to a high level of accuracy. However, it was also understood that certain freedoms are necessary based on accessibility of materials and limitations with manufacturing. The most important geometric concerns were the concentricity of the moderator and collimator and the thickness of the neutron absorbing material, which were both ensured.

The work proposed by Fantidis et al. did not specify void strength for the inside of the convergent moderator and divergent collimator. For the focus of this project, a vacuum within magnitudes of  $10^{-3}$  to  $10^{-1}$  Torr was assumed acceptable.

### 3.2 Design Creation

The majority of the physical design was done in three SolidWorks assemblies, roughly designed based on the parameters discussed in the previous section. With those parameters in mind, it was important to use concurrent engineering strategies to create a functional collimator within a set time frame. (Concurrent engineering is a technique that integrates design and development in such a way that they occur simultaneously. It is often used to shorten the time needed to create a product.) Additionally, it was important to approach the design with realistic manufacturing processes in mind, for the most time efficient completion.

The design was separated into the convergent moderator, the divergent collimator, the vacuum chamber, and subsequent supporting parts such as stands and chamber accessibility plates. The majority of the design work was completed using Dassault SolidWorks, Autodesk AutoCAD, and Autodesk Fusion 360.

The first portion of the design – the convergent moderator – was modelled in SolidWorks, and was then moved into Fusion 360 to create a CAM simulation, as shown in Figure 6.

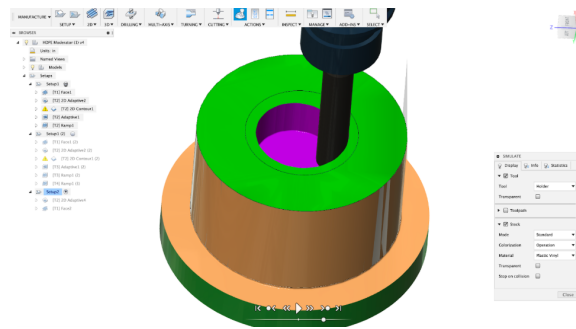


Figure 6: CAM simulation for convergent moderator

With manufacturability in mind, the part was redesigned to be manufactured into two separate 7 cm sections;

milling and turning a piece 14 cm in length, towards an inner taper of 1 cm, would not have been possible without custom tooling. Based on the part length, tapered geometry, and material it was concluded that the best method of manufacturing would be to vertically mill the plastic. A CNC Haas VM-2 was used to guarantee accurate dimensioning. The two parts were imported into Fusion 360 where CAM and milling simulations were carried out. The stock was then fixtured vertically in the VM-2, and was faced and milled to the specific OD to ensure dimensional accuracy (Figure 7). The inner conical shape was milled with a step of 0.01 in between layers, with a finishing path in between each layer with a ball endmill to create a smooth finish. The parts were then glued together with a polymer glue, and concentricity was ensured.

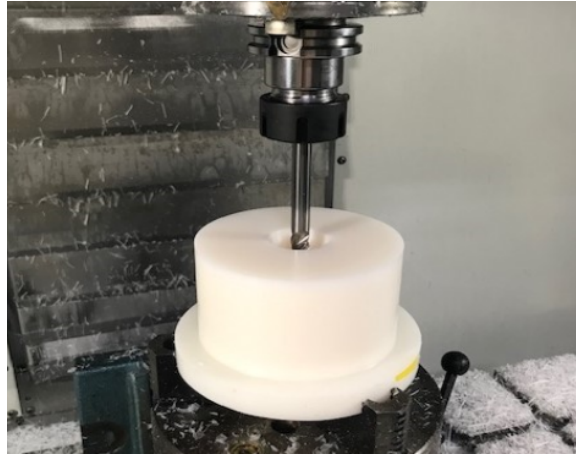


Figure 7: PE milling

The divergent collimator was the major design focus of the NR system. The cone-like shape and desired length proved to be a considerable challenge. It was decided that for cost reduction from already available material, time savings, and manufacturability that the divergent collimator section be designed as layered annuli, with varying inner and outer diameters, rather than as a whole cone. The 1 m in length was therefore split into 40 layers of 2.5 cm thick PPC-B, with a difference of 0.475 cm between the OD and ID of each layer, creating a beam divergence angle of  $4.57^\circ$  with reference to the beam port. The annuli were designed on SolidWorks using an Excel design table to create 40 configurations of the varying diameters. (See Appendix A.)

These layers were cut with a water-jet cutter, as laser cutting and/or milling posed the risk of melting the plastic, and outgassing boron particulates. Cookie-cutter assemblies of the configuration were devised to create a single .dxf file, with maximum annuli per sheet. These sheets were sent to an external machine shop with water-jet cutting capabilities. The water-jet ensured a tolerance of approximately 0.005 in on ID and OD dimensions. The next step in the manufacturing of the divergent collimator was to assemble each of the 40 layers into a cone shape. It was important to ensure the layers were stacked in the correct order, and were concentric. During assembly, each surface of a given layer of plastic was etched and covered with a two-part

plastic glue, and then pressed down onto an inner wooden stand. Wooden stands were laser cut to ensure that each layer was concentric. (See Appendix B.) The cone was glued into three separate sections for ease of transportation, inner stands were removed, and the three pieces were then glued together to complete the divergent collimator.

The final outlined section – the vacuum chamber – required exceptional attention to ensure a vacuum seal. Originally, a traditional prefabricated vacuum chamber design was researched, but a custom-made vacuum provided significant cost savings. Additionally, a custom-made vacuum chamber could be better tailored to project specifics and more easily maintained. Substantial cost savings were achieved by creating a rectangular chamber rather than a cylindrical one. The rectangular shape required four Al slabs to be sealed together however, which led to concerns on the quality of the vacuum seal. Originally, the strategy was to TIG weld the large Al plates together, but it was later discovered that welding sheets of 0.5 in thickness and 48 in length would be too challenging due to the lack of local heat at the point of the weld. For this reason, the plates were redesigned to include 12 tapped holes and countersunk mechanical fixturing points. The plates were designed to be sealed on one end by a welded end plate, and the other end with a gasket and an end plate, which was mechanically fixtured to a custom-made wide flange (Figures 8 and 9). The side plates were drilled and tapped in a VM-2 Haas Mini-Mill (Figure 10) in a total of four operations per plate, as each plate had to be shifted halfway through due to machine limitations on tool travel. The bottom plates were through-hole drilled and chamfer milled on the VM-2 machine to create 12 equally spaced 0.25 in countersunk screw holes, and were also done in a total of four operations per plate for similar tool restrictions. Additionally, one side plate was drilled and tapped to create a vacuum port inlet hole. This was done using a 13/16 drill and a 1 in tap on a manual drill press. While the outer plates were being machined, the end plates were outsourced to the same water-jet shop to more easily cut out the face geometry.

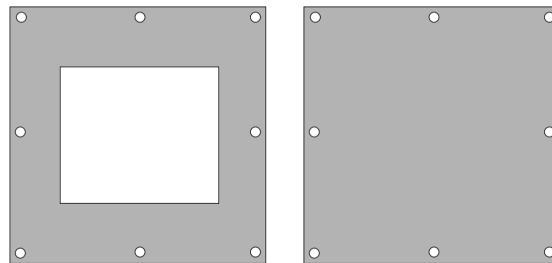


Figure 8: Vacuum chamber end plates

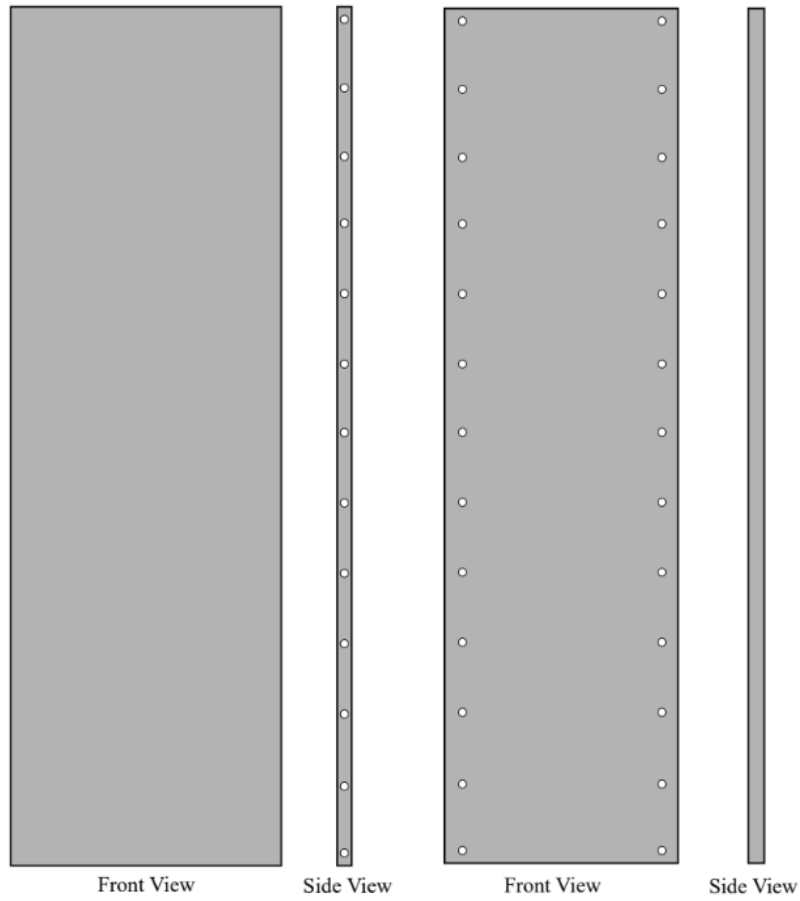


Figure 9: Side plates (left) and top and bottom plates (right)

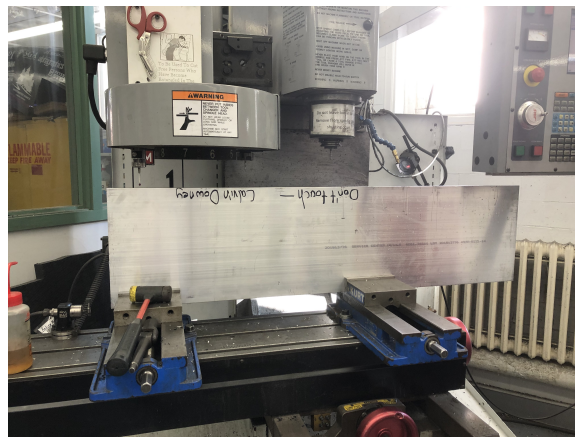


Figure 10: Side plate in a VM-2 Haas Mini-Mill

With each separate Al piece fully machined, the next step was to assemble the vacuum chamber. First, the plates were mechanically fixtured together with screws to examine warping of the plates and co-linearity of the tapped holes. The ends of the fixtured plates forming the body of the chamber were then grinded down at  $45^\circ$  angles to fit the end plates on flush for welding. It was important that the welds were thick enough

to maintain a vacuum seal around the edges. The edges of the chamber body – in between the top/bottom and side plates – were then covered with a sealant rated for high vacuum applications. The chamber also required a vacuum port, which was connected to an SD-91 vacuum. The port was drilled and then tapped with a 1 in -20 hole on one side of the chamber.

### 3.3 Neutron Activation Analysis

We completed two experiments to confirm flux values presented by Fantidis et al. which were found to be  $4.11\text{e}+3 \frac{\text{neutrons}}{\text{cm}^2\text{sec}}$ , with a TNC ratio of 3.88 [1],

$$\text{TNC} = \frac{\text{thermal neutron flux}}{\text{total neutron flux}}. \quad (8)$$

Flux was measured using two NAAs; one at a distance of 1 m away from the source without the collimator in place, and one at the same distance, except with the collimator in place. The NAA was completed by measuring thermal neutron irradiation of a sample,

$$A_o = N\sigma\phi Y(1 - e^{-\lambda t_i}), \quad (9)$$

where N is the number of target atoms,  $\sigma$  is the thermal neutron absorption cross-section [ $\text{cm}^2$ ],  $\phi$  is the neutron flux [ $\text{cm}^{-2}\text{s}^{-1}$ ],  $\lambda$  is the decay constant [ $\text{s}^{-1}$ ], Y is the fractional gamma yield, and  $t_i$  is the time of irradiation. After a gold foil sample was irradiated by the neutron generator for a set time frame (5 hours),  $\gamma$ -ray counts of the activated sample were measured using a HPGe detector, where counts are related to activity by,

$$C = \frac{A_o\epsilon}{\lambda} e^{-\lambda t_d}(1 - e^{-\lambda t_c}), \quad (10)$$

where  $\epsilon$  is the detector efficiency,  $t_d$  is the delay time before counting [s], and  $t_c$  is counting time [s]. Thermal flux was then determined using the known mass of the gold foil [15],  $m_{Au}$ ,

$$\Phi = \frac{C\lambda M_{Au}}{m_{Au} N_A \epsilon \sigma (1 - e^{-\lambda t_i}) e^{-\lambda t_d} (1 - e^{-\lambda t_c})}. \quad (11)$$

This test was first completed without the collimator in place. In preparation for the second round of testing, all of the manufactured pieces were assembled into the completed collimator system. (See Appendix C.) Wooden stands were laser cut to hold both the convergent moderator and the divergent moderator centered within the vacuum chamber. The stands were designed so that they would fit flush against the

convergent moderator and against specific pieces of the divergent collimator. The vacuum chamber was set to lay adjacent to the neutron generator and centered on the beam port. A gold foil was then centered onto the end of the collimator, to measure the most direct beam of neutrons.

## 4 Results and Discussion

### 4.1 Design Realization

The design of the collimator system was separated into the PE convergent moderator, the PPC-B divergent collimator, the Al vacuum chamber, and supporting parts to ensure functionality. Each part was designed and manufactured separately, and then assembled together to create the overall completed system.

The PE convergent collimator was faced to an OD of 13 cm, cut to 14 cm in length, and milled to have a tapered ID of 7 cm to 1 cm. It was found that splitting the manufacturing process into two separate pieces, each 7 cm in length, did not have any noticeable negative effects on the final product; the two pieces were glued together, and were found to be sufficiently concentric. The design is shown in Figure 11.

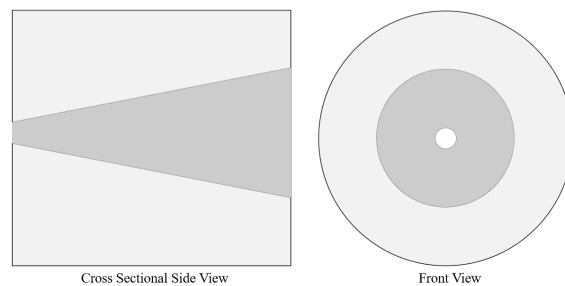


Figure 11: Moderator design

The divergent collimator required the most redesign, conceptualization, and assembly of individual pieces out of the system, and therefore had the most room for error. Each annuli was cut to the correct size, and stacked in the correct order to ensure the required cone-like shape would be attained. Additionally, although the inner wooden stands (Appendix B) proved helpful to ensure that the rings were glued in the correct position, they were difficult to remove once the glue dried, and were no longer necessary. As stated, the divergent collimator was initially assembled into three separate sections. The smallest of the three sections broke apart in a few areas between annuli while the stand was being removed. This section therefore had to be re-glued, with a new inner wooden stand in place. The three completed sections were then glued together without stands, so positioning at these two locations is likely off by a negligible amount. The cone was found to have both the desired length of 1 m, and a divergence angle of  $4.57^\circ$ . Figure 12 shows the inside of the completed divergent collimator.



Figure 12: Divergent collimator

The vacuum chamber also required exceptional attention to detail. The front of the chamber and an end fixturing plate were welded on, which ensured a vacuum seal at the ends, as shown in Figure 13.



Figure 13: TIG welds on vacuum chamber

Although a stitch weld was considered, a seam weld was used to ensure vacuum durability. The screw holes were found to be functional, and the plates experienced negligible warping. With the welds complete and screws in place, the sealant glue was placed in between the side plates, and the vacuum port was attached to the SD-91 vacuum, which fit flush against the chamber. The entire system was then assembled (Figure 14): wooden stands held the PE and PPC-B at the correct height within the chamber, and a rubber gasket in between the welded end fixture and the end plate ensured that the end of the collimator was sealed. Pb

blankets will surround the assembly whenever it is used to image.



Figure 14: Final collimator assembly

Although no major issues were encountered when assembling the collimator, areas of improvement were identified. It was noted that the glue used to merge together the annuli occasionally failed during assembly, and caused some annuli to not be perfectly flush. For future improvements, a different glue could be used, or the same glue could be applied more carefully. Additionally, although a cone-like shape was achieved, the final product was not perfectly smooth, and had steps in between annuli where the ID and OD changed. These areas could be sanded down in the future, which would have the potential to decrease neutron scattering, and therefore improve image quality. The divergent collimator was also built with PPC-B, although the material suggested by Fantidis et al. was PE-B. Fantidis et al. also suggested that the convergent moderator be filled with either a sapphire crystal or a void. This project uses a void, due to time and cost constraints. A sapphire may be placed inside of the convergent moderator in the future, however, if the TNC is too low without it [1].

## 4.2 Thermal Neutron Flux Analysis

Thermal neutron flux was measured with and without the collimator in place using NAA techniques. For each case, a gold foil was irradiated with neutrons for several hours, at approximately 1 m away from the generator.  $\gamma$ -ray counts were also measured using a high purity germanium detector, which allowed us to determine the flux of the beam. Counts were displayed using the spectroscopy software Genie 2000.

It was expected that Genie 2000 would display a peak at 411 keV, indicating the change from  $^{197}\text{Au}$  to  $^{198}\text{Au}$  due to neutron absorption from the generator [5]. However, upon inspection, it was found that this peak did not exist for either trial. This indicated that the neutron beam from the generator was not strong enough to reach the gold foils to cause a measurable change in mass. It was therefore hypothesized that the neutron generator was not functioning properly, and would have to be inspected before the collimator could be accurately characterized.

## 5 Conclusions

For this project we designed, manufactured, and assembled a compact neutron beam collimator for the WPI NSE neutron generator. The goals of this project were to

- fabricate a low cost collimator using replicable methods, and to make it customizable to a specific beam source and application,
- use concurrent engineering concepts to complete manufacturing within an academic school year,
- achieve an image plane flux of greater than  $10^6 \frac{\text{neutrons}}{\text{cm}^2 \text{sec}}$ , with a favorable TNC ratio, and
- outline future developments and applications of the collimator system.

The design of the collimator system was predominantly based on the MCNP parameter optimizations from Fantidis et al., and major geometric and material parameters were identified. It was decided to use already available materials as much as possible and to machine a custom vacuum chamber rather than to purchase a prefabricated chamber, both due to cost constraints. The choice to manufacture the vacuum chamber provided a 50% cost reduction when compared to the prefabricated setup, and the usage of PPC-B over PE-B provided between \$1000-\$1500 of savings. It was assumed that most NSE departments interested in creating a compact collimator would have this material, or a similar material, readily available. The system was designed with minimal parts and a straightforward assembly to be easily replicated; geometric parameters could be altered to fit specific applications and requirements (e.g. change in collimation ratio).

Concurrent engineering concepts were applied throughout manufacturing, and design changes were implemented throughout the manufacturing processes as necessary. For instance, it was found that it was not realistic to weld the lengths of the vacuum chamber walls, so the part was redesigned to be mechanically fixtured and sealed on the outside edges. Additionally, it was also found that inner stands would be necessary to ensure the concentricity of the divergent collimator. After assembly we then tested and outlined steps to characterize the collimator. These tests were useful, as our design varied slightly from the theoretical design from Fantidis et al.

Although the tests necessary to characterize the collimator were completed, our results were inconclusive. For the activation analyses, a gold foil was irradiated for five hours without the collimator, and another was irradiated for three hours with the collimator. For both runs, there was no evidence of a peak, meaning neutron flux was too low to activate the gold foils. Since the test was inconclusive for both runs, it was decided that the error stemmed from the neutron generator. Specifically, it was hypothesized that the turbopump within the generator was not operating properly, which caused the beam to arc whenever amperage went above 7mA. Ideally, the amperage of the beam at the target should be approximately 20-25 mA during operation to produce optimum fluxes. Therefore, future work is still needed to characterize the collimator; successful gold foil activation analyses will quantify the scattering ratio as well as the resulting flux at the image plane.

This project can be expanded and improved upon for students interested in NSE. In addition to collimator characterization, areas of future work include

- research and analysis of the use of quartz or sapphire crystal to filter out remaining fast neutrons,
- redesign of vacuum chamber to improve seal and material efficiency,
- recreation of divergent collimator stands with a less brittle and more warp resistant material, such as machined Al,
- alteration of the divergent collimator to be more geometry specific by smoothing steps in between layers, and
- research into the possible differences in neutron absorption and scattering cross-sections between PPC-B and PE-B.

The collimator should also be used for NR, to produce images with resolutions within 10 microns of magnitude.

## 6 References

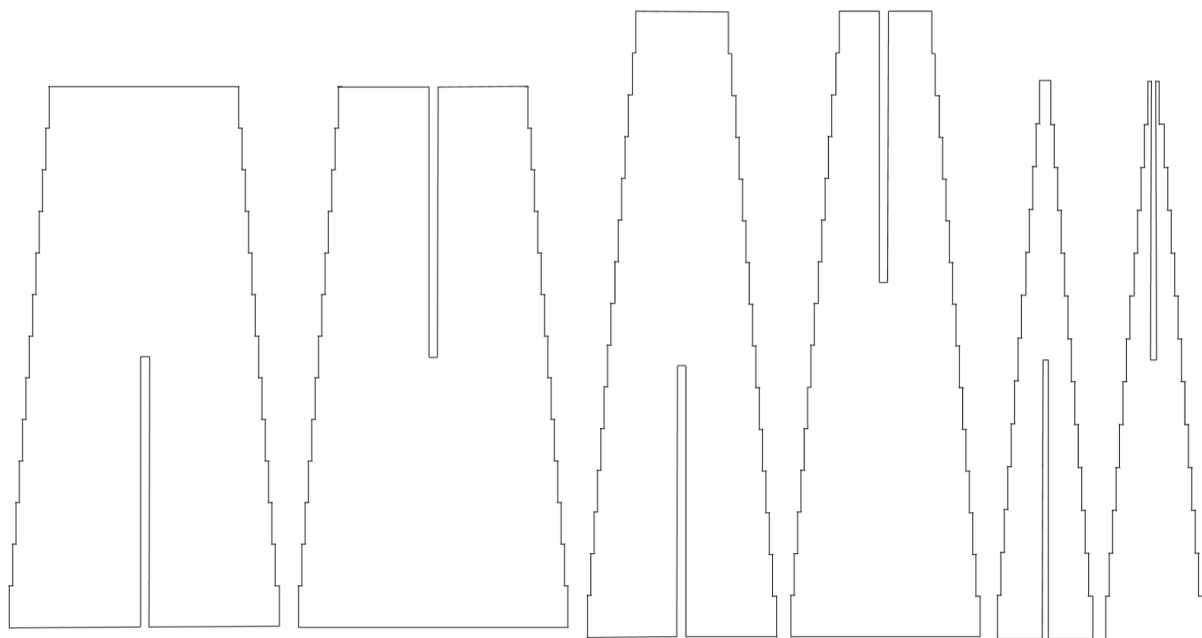
1. Fantidis et al.: Fast and thermal neutron radiographies based on a compact neutron generator. *Journal of Theoretical and Applied Physics* 2012 6:20.
2. The McClellan Nuclear Research Center. (n.d.). Retrieved April 10, 2019, from <https://mnrc.ucdavis.edu/neutron-radiography>.
3. Kardjilov, Nikolay Manke, Ingo Woracek, Robin Hilger, André Banhart, John. (2018). *Advances in neutron imaging. Materials Today*. 10.1016/j.mattod.2018.03.001.
4. Issard, H. (2015). Radiation protection by shielding in packages for radioactive materials (pp. 123-140).
5. Shultis, J. K., Faw, R. E. (2017). *Fundamentals of nuclear science and engineering* (pp. 161-188).
6. Neutron Energy. (n.d.). Retrieved from <https://www.nuclear-power.net/nuclear-power/reactor-physics/atomic-nuclear-physics/fundamental-particles/neutron/neutron-energy/>
7. Average Logarithmic Energy Decrement (n.d.) Retrieved from <https://www.nuclear-power.net/glossary/neutron-moderatoraverage-logarithmic-energy-decrement/>
8. "DD110 Neutron Generator." DD109-DD110 Neutron Generator – Adelphi Technology, Adelphi Technologies, [www.adelphitech.com/products/dd110.html](http://www.adelphitech.com/products/dd110.html).
9. J. Csikai, *Handbook of Fast Neutron Generators*, CRC Press, Inc., Boca Raton, Florida, USA, (1987)
10. Lou, T. (2003, May 1). Compact D-D/D-T neutron generators and their applications [Scholarly project]. Retrieved from <https://escholarship.org/uc/item/6213v5zq>
11. *J. Appl. Cryst.* (2012). 45, 1109-1124 <https://doi.org/10.1107/S0021889812041039>
12. Pleinert, Lehmann, et al. (1997, Nov. 11). Design of a new CCD-camera neutron radiography detector. [https://doi.org/10.1016/S0168-9002\(97\)00944-3](https://doi.org/10.1016/S0168-9002(97)00944-3).
13. KOBAYASHI, H. (n.d.). Design and Basic Character of Neutron Collimator on Radiography. *Japan Atomic Energy Research Institute*, 367-369. Retrieved April 10, 2019, from <https://inis.iaea.org/collection/NCLCollectionStore/Public/31/009/31009650.pdf>.
14. Taylor, Michael, et al. Thermal Neutron Radiography Using a High-Flux Compact Neutron Generator. *Physics Procedia*, vol. 88, 2017, pp. 175–183., doi:10.1016/j.phpro.2017.06.024.
15. R.C. Koch, CHAPTER 3 - ACTIVATION ANALYSIS EXPERIMENTAL METHODS, Editor(s): R.C. Koch, *Activation Analysis Handbook*, Academic Press, 1960, Pages 11-15, ISBN 9780123955098, <https://doi.org/10.1016/B978-0-12-395509-8.50007-5>.

## Appendix A: Cone Configurations

Table 1: Cone Configurations

Annulus Number	Inner Diameter	Outer Diameter	Inner Diameter	Outer Diameter
	[cm]	[cm]	[in]	[in]
1	1.00	9.00	0.39	3.37
2	1.38	9.38	0.54	3.51
3	1.75	9.75	0.69	3.65
4	2.13	10.13	0.84	3.79
5	2.50	10.50	0.98	3.93
6	2.88	10.88	1.13	4.07
7	3.25	11.25	1.28	4.21
8	3.63	11.63	1.43	4.35
9	4.00	12.00	1.57	4.49
10	4.38	12.38	1.72	4.63
11	4.75	12.75	1.87	4.77
12	5.13	13.13	2.02	4.91
13	5.50	13.50	2.17	5.05
14	5.88	13.88	2.31	5.19
15	6.25	14.25	2.46	5.33
16	6.63	14.63	2.61	5.47
17	7.00	15.00	2.76	5.61
18	7.38	15.38	2.90	5.75
19	7.75	15.75	3.05	5.89
20	8.13	16.13	3.20	6.03
21	8.50	16.50	3.35	6.17
22	8.88	16.88	3.49	6.31
23	9.25	17.25	3.64	6.45
24	9.63	17.63	3.79	6.59
25	10.00	18.00	3.94	6.73
26	10.38	18.38	4.08	6.87
27	10.75	18.75	4.23	7.01
28	11.13	19.13	4.38	7.15
29	11.50	19.50	4.53	7.29
30	11.88	19.88	4.68	7.43
31	12.25	20.25	4.82	7.57
32	12.63	20.63	4.97	7.71
33	13.00	21.00	5.12	7.85
34	13.38	21.38	5.27	7.99
35	13.75	21.75	5.41	8.13
36	14.13	22.13	5.56	8.27
37	14.50	22.50	5.71	8.41
38	14.88	22.88	5.86	8.55
39	15.25	23.25	6.00	8.69
40	15.63	23.63	6.15	8.83
41	16.00	24.00	6.30	8.97

## Appendix B: Inner Stands to Ensure Coincidence of Divergent Collimator



## Appendix C: Collimator Assembly

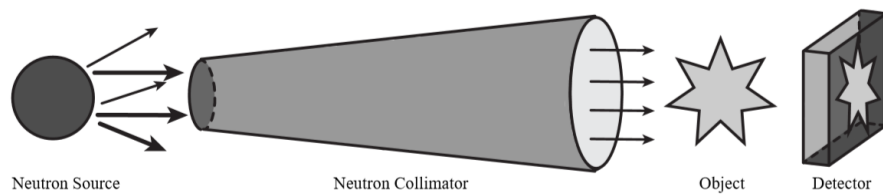


Figure C1: Basic neutron imaging setup



Figure C2: PE moderator with wooden stands placed inside of vacuum chamber



Figure C3: Collimator covered in Pb blankets to shield from unwanted radiation